Published in final edited form as:
Biomech Model Mechanobiol. 2010 October ; 9(5): 651–658. doi:10.1007/s10237-010-0194-x.

Characterizing the mechanical contribution of fiber angular distribution in connective tissue: comparison of two modeling approaches

Daniel H. Cortes,
McKay Orthopaedic Research Laboratory, Department of Orthopaedic Surgery, University of Pennsylvania, 424 Stemmler Hall, Philadelphia, PA 19104-6081, USA

Spencer P. Lake,
McKay Orthopaedic Research Laboratory, Department of Orthopaedic Surgery, University of Pennsylvania, 424 Stemmler Hall, Philadelphia, PA 19104-6081, USA

Jennifer A. Kadlowec,
McKay Orthopaedic Research Laboratory, Department of Orthopaedic Surgery, University of Pennsylvania, 424 Stemmler Hall, Philadelphia, PA 19104-6081, USA; Mechanical Engineering Department, Rowan University, Glassboro, NJ, USA

Louis J. Soslowsky, and
McKay Orthopaedic Research Laboratory, Department of Orthopaedic Surgery, University of Pennsylvania, 424 Stemmler Hall, Philadelphia, PA 19104-6081, USA

Dawn M. Elliott
McKay Orthopaedic Research Laboratory, Department of Orthopaedic Surgery, University of Pennsylvania, 424 Stemmler Hall, Philadelphia, PA 19104-6081, USA
delliott@mail.med.upenn.edu

Abstract

Modeling of connective tissues often includes collagen fibers explicitly as one of the components. These fibers can be oriented in many directions; therefore, several studies have considered statistical distributions to describe the fiber arrangement. One approach to formulate a constitutive framework for distributed fibers is to express the mechanical parameters, such as strain energy and stresses, in terms of angular integrals. These integrals represent the addition of the contribution of infinitesimal fractions of fibers oriented in a given direction. This approach leads to accurate results; however, it requires lengthy calculations. Recently, the use of generalized structure tensors has been proposed to represent the angular distribution in the constitutive equations of the fibers. Although this formulation is much simpler and fewer calculations are required, such structure tensors can only be used when all the fibers are in tension and the angular distribution is small. However, the amount of error introduced in these cases of non-tensile fiber loading and large angular distributions have not been quantified. Therefore, the objective of this study is to determine the range of values of angular distribution for which acceptable differences (less than 10%) between these two formulations are obtained. It was found, analytically and numerically, that both formulations are equivalent for planar distributions under equal-biaxial stretch. The comparison also showed, for other loading conditions, that the differences decrease when the fiber distribution is very small. Differences of less than 10% were usually obtained when the fiber distribution was very low ($\kappa \approx 0.03$; κ ranges between 0 and 1/3, for aligned and isotropic distributed fibers, respectively). This range of angular distribution

Correspondence to: Dawn M. Elliott.

greatly limits the types of tissue that can be accurately analyzed using generalized structure tensors. It is expected that the results from this study guide the selection of a proper approach to analyze a particular tissue under a particular loading condition.

Keywords

Connective tissue; Collagen fibers; Fiber angular distribution; Structure tensors

1 Introduction

Collagen fibers are the principal component of connective tissues. The role of the fibers is mainly mechanical, providing the tissue with the required stiffness and strength. These fibers are loaded in tension and buckle under compression (Holzapfel et al. 2004). Therefore, the mechanical behavior of connective tissues in tension is influenced by fiber structural arrangement. For instance, in tendons, where the main function is to transmit loads from muscle to bone, the collagen fibers are mostly aligned along the tendon's long axis. Another example can be found in intervertebral discs, where fibers of the annulus fibrosus are oriented in multiple directions to support a multiaxial loading environment. A variety of modeling approaches incorporate collagen fibers explicitly as one of the components. Therefore, connective tissues are often analyzed as a fiber-reinforced composite material (Spencer 1984). However, due to the complexity of the fiber organization, simplified geometries are usually considered (Diamant et al. 1972; Comninou and Yannas 1976; Lanir 1978). Tissue modeling studies generally assume perfectly aligned fibers (Spilker et al. 1992; Limbert and Middleton 2004), although some studies have utilized a discrete number of fiber directions to represent fiber architecture (Wu and Yao 1976; Holzapfel et al. 2000; Garcia 2007; Guerin and Elliott 2007). In the pioneering work of Lanir, a constitutive relation for continuous fiber distributions was proposed (Lanir 1983) and it has been applied for a variety of tissues such as articular cartilage, arteries and aortic valves (Ateshian et al. 2009; Sacks 2003; Freed et al. 2005; Gasser et al. 2006).

The strain energy and stresses, for a continuous fiber distribution, can be obtained by angular integration (AI) of infinitesimal fractions of fibers aligned in a given direction. This formulation allows the use of any angular distribution (experimental values or mathematical function) and constitutive model for the fibers. Additionally, the assumption that fibers are only loaded in tension can be easily implemented in this method. Several special cases of this theory have been successfully used to describe the mechanical behavior of a variety of tissues (Lanir et al. 1996; Billiar and Sacks 2000; Sacks 2003; Nguyen et al. 2008; Girard et al. 2009; Ateshian et al. 2009; Pandolfi and Holzapfel 2008). In particular, Ateshian et al. (2009) showed that large values of the tensile Poisson's ratio for articular cartilage in tension and the low values observed in compression can only be explained using a continuous angular distribution for the fibers. Since this approach leads to accurate results, it can be considered the ‘gold standard’. However, a disadvantage of the AI formulation is the large number of calculations required to evaluate the strain and stresses.

Generalized structure tensors (GST) have been recently proposed for the modeling of tissues with continuously distributed collagen fibers (Freed et al. 2005; Gasser et al. 2006). These tensors are a mathematical entity assumed to represent the three-dimensional distribution of the fibers. Once the tensor has been defined, the strain in the fibers can be readily obtained by a multiplication with a strain tensor. The popularity of this approach lies in the small number of calculations required to obtain the strain energy and stresses of the fibers. Therefore, this formulation can be efficiently implemented in numerical algorithms like finite elements. Federico and Herzog (2008) elegantly demonstrated that this approach is valid only when all

the fibers are in tension and when the fiber distribution is small. However, the amount of error introduced in these cases of non-tensile fiber loading and large angular distributions have not been quantified. A numerical comparison between these methods is required to determine when differences can be considered small enough to permit use of the more computationally efficient GST method.

The objective of this study is to quantitatively compare the AI and GST formulations to determine the range of values of angular distribution for which the GST approach can be used. To this end, the differences between these approaches are initially derived analytically and then illustrated numerically as a function of the angular distribution for several loading conditions. It is expected that this study will provide guidance to select the appropriate approach to model a particular tissue under a given loading environment.

2 Angular integration and generalized structure tensors formulations

2.1 Angular integration (AI)

In Lanir's formulation, the fiber distribution was described by a spatial density distribution function, which quantifies the volumetric fraction of fibers oriented in a particular direction. The total strain energy and stresses were calculated as the integration of the energy and stresses of fibers in all directions. This general formulation was later simplified for the case of planar tissues under biaxial testing (Lanir et al. 1996). Similar approaches were presented by Ateshian et al. (2009), Girard et al. (2009), Nguyen et al. (2008), Billiar and Sacks (2000) and Sacks (2003).

In general, the strain energy (Ψ) and the second Piola-Kirchhoff stress tensor ($\mathbf{S}_f$) for a family of distributed fibers can be expressed as

$$\Psi_f = \int_\Omega \rho(\theta,\varphi)\overline{\Psi}(\lambda)\mathrm{d}\Omega \tag{1a}$$

$$\mathbf{S}_f = 2\frac{\partial \Psi_f}{\partial \mathbf{C}} = 2\int_\Omega \rho(\theta,\varphi)\frac{\partial \overline{\Psi}(\lambda)}{\partial \mathbf{C}}\mathrm{d}\Omega, \tag{1b}$$

where $\rho(\theta, \varphi)$ is the density distribution function, θ and φ are Eulerian angles describing the direction of any spatial vector (Fig. 1), λ is the stretch of a fiber, $\overline{\Psi}$ is the strain energy of a fiber, $\mathbf{C}$ is the right Green-Cauchy strain tensor, Ω is the surface of a unit sphere and $\mathrm{d}\Omega = \sin\theta \mathrm{d}\theta \mathrm{d}\varphi$. In Eq. (1), it is assumed that the fiber will buckle under any compressive deformation; therefore, $\overline{\Psi}(\lambda) = 0$ and $\partial\overline{\Psi}(\lambda)/\partial\mathbf{C} = 0$ for $\lambda \leq 1.0$. The partial derivative in Eq. (1b) can be rewritten using the chain rule as

$$\frac{\partial \overline{\Psi}}{\partial \mathbf{C}} = \frac{\partial \overline{\Psi}}{\partial \lambda}\frac{\partial \lambda}{\partial \mathbf{C}} = \frac{1}{2\lambda}\frac{\partial \overline{\Psi}}{\partial \lambda}\mathbf{M}\otimes\mathbf{M}, \tag{2}$$

where $\mathbf{M}$ is an unit vector representing the average direction of an infinitesimal fraction of fibers, and the stretch, in the direction $\mathbf{M}$, is related to the strain tensor by $\lambda^2 = \mathbf{C}:\mathbf{M}\otimes\mathbf{M}$. Therefore, Eq. (1b) can be rewritten as

$$\mathbf{S}_{\mathrm{f}}=2\frac{\partial\Psi_{\mathrm{f}}}{\partial\mathbf{C}}=2\int_{\Omega}\rho(\theta,\varphi)\frac{1}{2\lambda}\frac{\partial\overline{\Psi}}{\partial\lambda}\mathbf{M}\otimes\mathbf{M}\mathrm{d}\Omega. \tag{3}$$

Equation (3) is valid for a general 3-dimensional fiber distribution. However, it can be simplified for the case of planar fiber distributions as

$$S_{\mathrm{f}}=2\int_{0}^{\pi}\rho(\theta)\frac{1}{2\lambda}\frac{\partial\overline{\Psi}}{\partial\lambda}\mathbf{M}\otimes\mathbf{M}\mathrm{d}\theta. \tag{4}$$

Although Eq. (4) has been solved for a particular choice of $\rho(\theta)$ and $\overline{\Psi}$ (Raghupathy and Barocas 2009), in general, it is very difficult to obtain a closed-form solution; therefore, numerical integration is the usual alternative.

2.2 Generalized structure tensors (GST)

Structure tensors are an alternative approach to formulate the constitutive relations for fiber-reinforced materials. For a material with perfectly aligned fibers, the structure tensor can be defined as the dyadic product $\mathbf{a}_0 \otimes \mathbf{a}_0$, where $\mathbf{a}_0$ is a unit vector in the direction of the fibers in the reference configuration. The strain energy can be expressed as a function of the invariants of $\mathbf{C}$ and $\mathbf{a}_0 \otimes \mathbf{a}_0$

$$I_1=\mathbf{C}:\mathbf{I}, I_2=1/2\left\{tr^2\mathbf{C}-tr\mathbf{C}^2\right\}, I_3=det\ \mathbf{C},$$
$$I_4=\mathbf{C}:\mathbf{a}_0\otimes\mathbf{a}_0. \tag{5}$$

A general discussion on the use of these invariants and tensors can be found in Spencer (1984). Recently, Freed et al. (2005) and Gasser et al. (2006) formulated GSTs, which consider the effect of fiber angular distribution. The angular distribution tensor ($\mathbf{H}$) is defined as

$$\mathbf{H}=\int_{\Omega}\rho(\theta,\varphi)\mathbf{M}\otimes\mathbf{M}\mathrm{d}\Omega. \tag{6}$$

Notice that $\mathbf{M}$ represents the direction of an infinitesimal fraction of fibers and it is used inside integral expressions and $\mathbf{a}_0$ represents global fiber orientations. Again, Eq. (6) can be simplified for planar fiber distributions as

$$\mathbf{H}=\int_{0}^{\pi}\rho(\theta)\mathbf{M}\otimes\mathbf{M}\mathrm{d}\theta. \tag{7}$$

The pseudo-invariant $I_{\langle 4\rangle}=\mathbf{C}:\mathbf{H}$, can be expressed in an integral form, using Eq. (6), as

$$I_{\langle 4\rangle}=\mathbf{C}:\int_{\Omega}\rho(\theta,\varphi)\mathbf{M}\otimes\mathbf{M}\mathrm{d}\Omega=\int_{\Omega}\rho(\theta,\varphi)\mathbf{C}:\mathbf{M}\otimes\mathbf{M}\mathrm{d}\Omega$$
$$=\int_{\Omega}\rho(\theta,\varphi)\lambda^2\mathrm{d}\Omega=\overline{\lambda}^2. \tag{8}$$

A similar expression can be easily obtained for planar distributions. From Eq. (8), it can be observed that $I_{\langle 4\rangle}$ is the weighted average of λ^2. Notice that in the definition of $I_{\langle 4\rangle}$, there is not a condition to exclude fibers under compression. Therefore, if one of the principal values of **C** is lower than 1.0, a fraction of compressed fibers will be included in the average $\overline{\lambda}^2$. Uniaxial tension, biaxial tension and simple shear are examples of deformation states for which at least one of the principal values of **C** is less than one. Consequently, error will be introduced when the GST formulation is considered in these loading scenarios.

For the generalized structural tensor, the strain energy (Ψ_f) and the second Piola-Kirchhoff ($\mathbf{S}_f$) stress tensor can be expressed as

$$\Psi_f=\overline{\Psi}\left(\overline{\lambda}\right), \tag{9a}$$

$$\mathbf{S}_f=2\frac{\partial\overline{\Psi}}{\partial\mathbf{C}}=\frac{1}{\overline{\lambda}}\frac{\partial\overline{\Psi}}{\partial\overline{\lambda}}\frac{\partial\overline{\lambda}}{\partial\mathbf{C}}=\frac{1}{\overline{\lambda}}\frac{\partial\overline{\Psi}}{\partial\overline{\lambda}}\mathbf{H}. \tag{9b}$$

An essential difference between the AI and GST is that, for the GST, the strain energy function and the stresses are calculated using the average stretch rather than the actual stretch in the fibers. In general, lower stresses are obtained when $\overline{\lambda}$ is used in the constitutive equations.

3 Particular cases and comparison between AI and GST formulations

In this section, both formulations are compared analytically in a general form without specifying a constitutive equation for the fibers. Although Federico and Herzog (2008) also presented an analysis of the differences between these two formulations, in this section we are comparing a few cases for which analytical solutions can be easily calculated. Three cases will be considered: two for which the formulations are equivalent (perfectly aligned fibers and constant fiber stretch) and one case in which they are different (isotropic fiber distribution). For perfectly aligned fibers, the distribution density function $\rho(\theta,\varphi)$ becomes the product of Dirac delta functions, $\delta(\theta)\,\delta(\varphi)$. Therefore, the stresses in the AI formulation (Eq. (3)) can be expressed as

$$\mathbf{S}_f=2\int_{\Omega}\delta(\theta)\delta(\varphi)\frac{1}{2\lambda}\frac{\partial\overline{\Psi}}{\partial\lambda}\mathbf{M}\otimes\mathbf{M}\mathrm{d}\Omega$$
$$=\frac{1}{\lambda_{\mathbf{a}_0}}\frac{\partial\overline{\Psi}}{\partial\lambda}\left(\lambda_{\mathbf{a}_0}\right)\mathbf{a}_0\otimes\mathbf{a}_0$$
$$=2\frac{\partial\overline{\Psi}}{\partial I_4}\mathbf{a}_0\otimes a_0 \tag{10}$$

where $\mathbf{a}_0$ is a unit vector in the fiber direction, and $I_4=\lambda^2_{\mathbf{a}_0}$. On the other hand, for the GST formulation, it can be easily shown from Eq. (6) that **H** becomes $\mathbf{a}_0\otimes\mathbf{a}_0$, and the pseudo-invariant $I_{\langle 4\rangle}$ tends to $I_4=\lambda^2_{\mathbf{a}_0}$. Therefore, the second P-K stress tensor can be expressed as

$$\mathbf{S}_f = 2\frac{\partial \overline{\Psi}}{\partial I_4}\mathbf{a}_0 \otimes \mathbf{a}_0. \tag{11}$$

The second case for which these two formulations coincide is when the stretch in the fibers is the same in all directions (i.e., dilatational loading). In this case, the average stretch, $\bar{\lambda}$, and the actual stretch of the fiber are the same; therefore, Eq. (3) can be expressed as

$$\mathbf{S}_f = 2\frac{1}{2\bar{\lambda}}\frac{\partial \overline{\Psi}}{\partial \bar{\lambda}}\int_\Omega \rho(\theta,\varphi)\mathbf{M}\otimes\mathbf{M}d\Omega = \frac{1}{\bar{\lambda}}\frac{\partial \overline{\Psi}}{\partial \bar{\lambda}}\mathbf{H}. \tag{12}$$

Notice that Eq. (12) is identical to Eq. (9b); therefore, the AI and GST formulations are equivalent for any angular distribution when the fiber stretch is uniform. A similar equivalency can be obtained for planar distributions under equibiaxial stretch.

A case where the formulations clearly differ is when the fiber distribution is isotropic, e.g., $\rho(\theta, \varphi)$ is constant. For GST, from Eq. (6), it can be observed that **H** becomes one third of the identity tensor, $\frac{1}{3}\mathbf{I}$, thus $I_{\langle 4\rangle} = \overset{-2}{\lambda} \rightarrow \frac{1}{3}I_1$. Therefore, Eq. (9) can be rewritten as

$$\Psi_f = \overline{\Psi}(I_1), \tag{13a}$$

$$\mathbf{S}_f = 2\frac{\partial \overline{\Psi}}{\partial \mathbf{C}} = \frac{2}{3}\frac{\partial \overline{\Psi}}{\partial I_1}\mathbf{I}. \tag{13b}$$

Consequently, for an isotropic fiber distribution, the fiber term predicts only constant normal stress in all directions.

4 Numerical comparison

It has been shown that both formulations lead to similar results when the fibers are in tension and the angular distribution is small (Federico and Herzog 2008). In the previous section, two cases were presented for which both formulations have the same analytical solution. The objective is to determine for which values of fiber distribution acceptable differences are obtained. To this end, a particular angular distribution and constitutive equation for the fibers have been chosen. Here, acceptable differences are defined to be within 10%. However, the comparisons are presented for the entire range of fiber distribution (e.g., from totally aligned to isotropic distributed fibers); therefore, the difference between formulations can be obtained for any value of the fiber distribution.

The following energy function has been chosen (Holzapfel et al. 2000) as a constitutive relation to describe the mechanical behavior of the collagen fibers

$$\overline{\Psi} = \frac{c_1}{2c_2}\left[e^{c_2(\lambda^2-1)^2} - 1\right]. \tag{14}$$

where c_1 is an elastic constant and c_2 a is non-dimensional parameter associated with the degree of nonlinearity. The total energy of the fibers can be calculated using Eq. (1a) or Eq. (9a) for the AI and GST formulations, respectively. For a transversely isotropic fiber distribution, the density function proposed by Gasser et al. (2006) was selected.

$$\rho(\theta)=\frac{1}{\pi}\sqrt{\frac{b}{2\pi}}\frac{e^{[b(\cos(2\theta)+1)]}}{erfi\left(\sqrt{2b}\right)}, \tag{15}$$

where b is called a concentration parameter (it is associated with the spread of the distribution function), and *erfi* is the imaginary error function. Notice that, although this fiber distribution (Eq. 15) is a function of only one angle, the fiber arrangement is 3-dimensional. The generalized structure tensor associated with this density function can be expressed as (Gasser et al. 2006)

$$\mathbf{H}=\kappa\mathbf{I}+(1-3\kappa)\mathbf{a}_0\otimes\mathbf{a}_0, \tag{16}$$

where $\kappa=2\pi\int_0^{\pi}\rho(\theta)\sin^3\theta\mathrm{d}\theta$ ranges from 0 to 1/3 for perfectly aligned and isotropic distributed fibers, respectively. An expression similar to Eq. (16) can be obtained for a planar (von Mises) distribution

$$\mathbf{H}_2=\kappa\mathbf{I}_2+(1-2\kappa)\mathbf{a}_{0_2}\otimes\mathbf{a}_{0_2}, \tag{17}$$

where $\mathbf{H}_2$, $\mathbf{I}_2$ and $\mathbf{a}_{0_2}\otimes\mathbf{a}_{0_2}$ are two-dimensional versions of the tensors shown in Eq. (16), the distribution parameter is now defined as $\kappa_{2D}=\int_0^{\pi}\rho(\theta)\sin^2\theta d\theta$ and ranges from 0 to 1/2. Figure 2 illustrates the von Mises distribution for two values of κ_{2D}. The shaded areas represent the angular range which contains 95% of the fibers; i.e., the ±26° and ±71.8° for κ_{2D} = 0.05 and 0.25, respectively.

Three loading configurations, typically used to characterize connective tissues, have been selected for comparison: uniaxial tension, biaxial tension, and simple shear. In order to determine the range of values of κ, an acceptable difference (100 * (S_{AI} − S_{GST})/S_{AI}) in the stresses of 10% was selected. Additionally, since the difference in the formulations depends on the applied stretch, a maximum stretch of 1.2 is chosen. This value of stretch is supposed to represent a typical range of deformation for connective tissue. A single set of material properties is used throughout this section: c_1 = 5MPa, c_2 = 30MPa. It is assumed that these properties describe the behavior of the supraspinatus tendon (Kadlowec et al. 2009). Finally, the tissue is considered as an incompressible material; therefore, the condition $det\mathbf{C}$ = 1 holds.

Figure 3 shows the comparison between the AI and GST formulations for planar (2D) and transversely isotropic (3D) distributions under uniaxial tension. First, notice that the behavior of the planar and the transversely isotropic distributions is similar. It can be observed that the difference between the AI and GST formulations tends to zero when the fibers are highly aligned ($\kappa \to 0$). This can be attributed to the reduced number of buckled fibers. A difference of 10% in the longitudinal stress is obtained for κ = 0.015 (κ_{2D} = 0.022) when a stretch of 1.2 is applied. If the stretch applied is 1.10, an acceptable (10%) difference is obtained when κ is lower than 0.043 (κ_{2D} = 0.065).

Several comparisons have been made to analyze the case of biaxial loading. Figure 4a shows the comparison between the AI and GST considering a von Mises (2D planar) fiber distribution. In this case, a stretch is applied in the mean direction of the fibers (λ_1) and the lateral direction is kept fixed (λ_2). In this loading configuration, none of the fibers experience buckling. However, the disparity between AI and GST obtained for this configuration can be attributed to using the average stretch instead of integrating the actual energy of the fibers. For example, for a value of κ equal to 0.03, a difference of 10% is obtained for S_{11} when a stretch of 1.2 is applied in the direction x_1.

To determine the effect of the strain configuration in the biaxial testing of planar (2D) family of fibers, a comparison between formulations as a function of the Lagrangian strain ratio E_{22}/E_{11} for several values of κ_{2D} is shown in Fig. 4b. In this plot, the ratio between stresses was calculated keeping the stretch in the direction x_1 constant and equal to 1.2. Therefore, the ratios $E_{22}/E_{11} = 0$ and $E_{22}/E_{11} = 1$ correspond to the transverse fixed and equal-biaxial configurations, respectively. It can be observed that the differences between formulations vanish for the case of equal-biaxial strains, regardless of the angular distribution. However, when the angular distribution is large (e.g., $\kappa_{2D} = 0.25$ or 0.5), small differences are obtained only when the strain configuration is close to equal-biaxial; i.e., a difference of 10% is obtained for $E_{22}/E_{11} = 0.96$ for $\kappa_{2D} = 0.5$.

Several tissues, like annulus fibrosus and arteries, have two families of fibers. Usually, it is assumed that both families have the same fiber properties and angular distribution (Yin and Elliott 2005). Figure 5a and b show the comparison between formulations for the stress component S_{11} in a biaxial test. For this comparison, a tissue with two planar (2D) fibers families oriented at ±30° from the axis x_1 was considered. Figure 5a shows that the stress difference as a function of κ_{2D} is similar to that for a single family of fibers (Fig. 4a); however, it can be observed that for low values of κ_{2D}, the stress difference is larger for the case of two fiber families. A difference of 10% is obtained for $\lambda_1 = 1.2$ and $\kappa_{2D} = 0.0026$. Also notice that the difference for isotropic fiber distribution ($\kappa_{2D} = 0.5$) is the same as that of a single family of fibers, as expected. On the other hand, Fig. 5b shows that the stress differences vanish for the case of equal-biaxial strain. Notice that the curves for isotropic distribution ($\kappa_{2D} = 0.5$) in Figs. 4b and 5b are identical.

It has been shown, analytically and numerically, that no difference between formulations exists when a planar (2D) fiber distribution is subjected to equal-biaxial stretch (Figs. 4b and 5b). However, if the fiber distribution is transversely isotropic (3D), as that of Eq. (15), a fraction of the fibers buckle due to the out-of-plane contraction and therefore do not contribute to total stresses in the tissue. However, in the GST formulation, those fibers are considered in the calculation of the average stretch. To illustrate this, a single fiber of families with transversely isotropic distribution under equal-biaxial stretch is analyzed. Figure 6 shows the stress difference as a function of fiber distribution for several values of the applied stretch. A 10% difference is obtained for $\kappa = 0.014$ and a stretch equal to 1.2. This value is very close to that obtained for the case of uniaxial tension (Fig. 3).

Finally, the case of simple shear is analyzed. From Eqs. (16) and (17), it can be noticed that if the main direction of the fiber is aligned with the axes x_1 or x_2, all the off-diagonal components of the generalized structure tensor **H** are zero. Therefore, there is no contribution of the fibers to the shear stresses in the case of GST. Conversely, from Eqs. (3) and (4), it is observed that the contribution of the fibers to the shear stresses is non-zero for the case of AI. Consequently, for these fiber orientations, the difference will be 100% for all values of fiber distribution. On the other hand, a comparison for a planar (2D) family of fibers oriented at 45° from x_1 under simple shear is shown in Fig. 7. Notice that fiber buckling occurs in the direction of the compressive principal strain. The differences between formulations are 0 or 100% when the

fibers are aligned ($\kappa_{2D} = 0$) or homogeneously distributed ($\kappa_{2D} = 0.5$), respectively. A difference of 100% for an isotropic distribution is expected, since the second term of the right hand side of Eq. (17) vanishes when $\kappa_{2D} = 0.5$. A 10% difference was obtained when $\kappa_{2D} = 0.02$ for E12 = 0.2.

5 Conclusions

This study provided quantitative comparisons between the constitutive frameworks using AI and GST to describe the mechanical behavior of connective tissues. While it has been established that under various loading conditions errors can be introduced in the structural tensor approach (Federico and Herzog 2008), this study quantified the difference between these two modeling frameworks to guide potentially appropriate applications for the more computationally efficient structural formulation. Several loading conditions, such as uniaxial, biaxial tension and simple shear, were considered. The differences were calculated as a function of angular distribution; therefore, the range of values of κ for which acceptable differences are obtained was determined. It was found, analytically and numerically, that both formulations are equivalent for planar distributions for the case equal-biaxial stretch. The comparison also showed, for other loading conditions, that the differences decrease when the fiber distribution is very small. Differences of less than 10% were usually obtained when the fiber distribution parameter was low ($\kappa \approx 0.03$). This comparison can be used as a guideline to choose the proper formulation for a given tissue and loading conditions.

Acknowledgments

This study was supported by a grant from the NIH/NIAMS (AR055598) and the NIH/NIAMS-supported Penn Center for Musculoskeletal Disorders (AR050950).

References

Ateshian G, Rajan V, Chahine NO, Canal CE, Hung CT. Modeling the matrix of articular cartilage using a continuous fiber angular distribution predicts many observed phenomena. J Biomech Eng 2009;131:061003. [PubMed: 19449957]

Billiar KL, Sacks MS. Biaxial mechanical properties of the native and glutaraldehyde-treated aortic valve cusp: part II—a structural constitutive model. J Biomech Eng 2000;122:327–335. [PubMed: 11036555]

Comninou M, Yannas IV. Dependence of stress-strain nonlinearity of connective tissues on the geometry of collagen fibers. J Biomech 1976;9:427–433. [PubMed: 939764]

Diamant J, Keller A, Baer E, Litt M, Arridge RGC. Collagen; ultrastructure and its relation to mechanical properties as a function of ageing. Proc R Soc Lond B 1972;180:293–315. [PubMed: 4402469]

Federico S, Herzog W. Towards an analytical model of soft biological tissues. J Biomech 2008;41:3309–3313. [PubMed: 18922533]

Freed AD, Einstein DR, Vesely I. Invariant formulation for dispersed transverse isotropy in aortic heart valves. Biomech Model Mechanobiol 2005;4:100–117. [PubMed: 16133588]

Garcia JJ. Simulation of tensile high Poisson's ratios of articular cartilage with a finite element fiber-reinforced hyperelastic model. Med Eng Phys 2007;30:590–598. [PubMed: 17690001]

Gasser TC, Ogden RW, Holzapfel GA. Hyperelastic modeling of arterial layers with distributed collagen fibre orientations. J R Soc Interface 2006;3:15–35. [PubMed: 16849214]

Girard MJA, Downs JC, Burgoyne CF, Francis-Suh JK. Peripapilary and posterior scleral mechanics part I: development of an anisotropic hyperelastic constitutive model. J Biomech Eng 2009;131:051011. [PubMed: 19388781]

Guerin HL, Elliott DM. Quantifying the contributions of structure to annulus fibrosus mechanical function using a nonlinear, anisotropic, hyperelastic model. J Orthop Res 2007;25:508–516. [PubMed: 17149747]

Holzapfel GA, Gasser TC, Ogden RW. A new constitutive framework for arterial wall mechanics and a comparative study of material models. J Elast 2000;61:1–48.

Holzapfel GA, Gasser TC, Ogden RW. Comparison of a multilayer structural model for arterial walls with a Fung-type model, and issues of material stability. J Biomech Eng 2004;126:264–275. [PubMed: 15179858]

Kadlowec, JA.; Lake, SP.; Miller, KS.; Soslowsky, LJ.; Elliott, DM. A hyperelastic model with distributed fibers to describe the human supraspinatus tendon tensile mechanics. Summer Bioengineering Conference; Lake Tahoe, CA. 2009.

Lanir Y. Structure-strength relations in mammalian tendon. Biophys J 1978;24:541–553. [PubMed: 728528]

Lanir Y. Constitutive equations for fibrous connective tissues. J Biomech 1983;16:1–12. [PubMed: 6833305]

Lanir Y, Lichtenstein O, Imanuel O. Optimal design of biaxial tests for structural material characterization of flat tissues. J Biomech Eng 1996;118:41–47. [PubMed: 8833073]

Limbert G, Middleton J. A transversely isotropic viscohyperelastic material: Application to the modeling of biological soft connective tissues. Int J Solids Struct 2004;41:4237–4260.

Nguyen TD, Jones RE, Boyce BL. A nonlinear anisotropic viscoelastic model for the tensile behavior of the corneal stroma. J Biomech Eng 2008;130:041020. [PubMed: 18601462]

Pandolfi A, Holzapfel GA. Three-dimensional modeling and computational analysis of the human cornea considering distributed collagen fibril orientations. J Biomech Eng 2008;130:061006. [PubMed: 19045535]

Sacks MS. Incorporation of experimentally-derived fiber orientation into a structural constitutive model for planar collagenous tissues. J Biomech Eng 2003;125:187–280.

Spencer, AJM. Continuum theory of the mechanics of fibre-reinforced composites. Springer; New York: 1984.

Spilker RL, Donzelli PS, Mow VC. A transversely isotropic biphasic finite element-model of the meniscus. J Biomech 1992;25:1027–1045. [PubMed: 1517263]

Raghupathy R, Barocas VH. A closed-form structural model of planar fibrous tissue mechanics. J Biomech 2009;42:1424–1428. [PubMed: 19457487]

Wu HC, Yao RF. Mechanical behavior of human annulus fibrosus. J Biomech 1976;9:1–7. [PubMed: 1249075]

Yin LA, Elliott DM. A homogenization model for the annulus fibrosus. J Biomech 2005;38:1674–1684. [PubMed: 15958225]

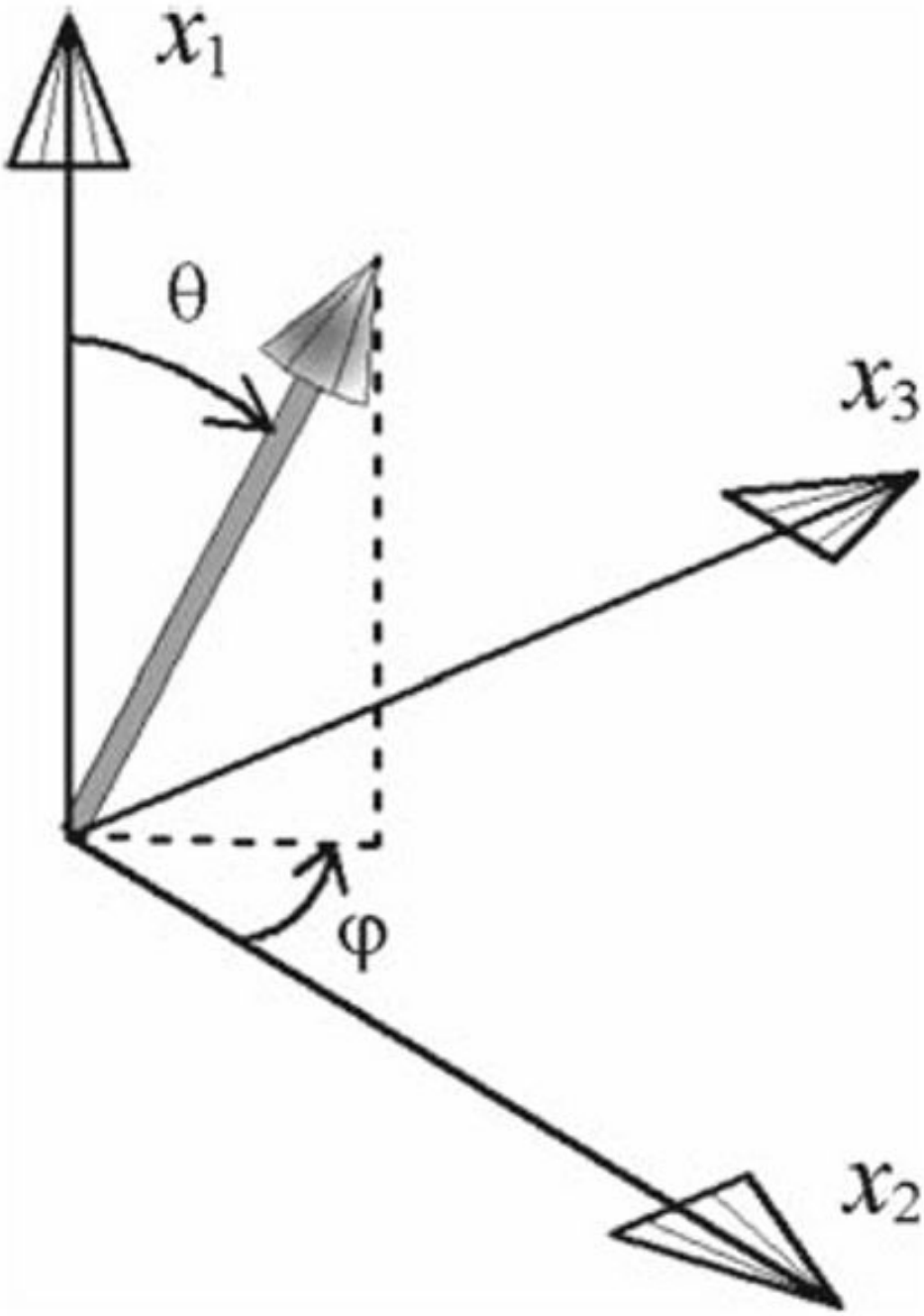

Fig. 1.
Eulerian angles used to define the direction of a vector in a 3-dimensional coordinate system

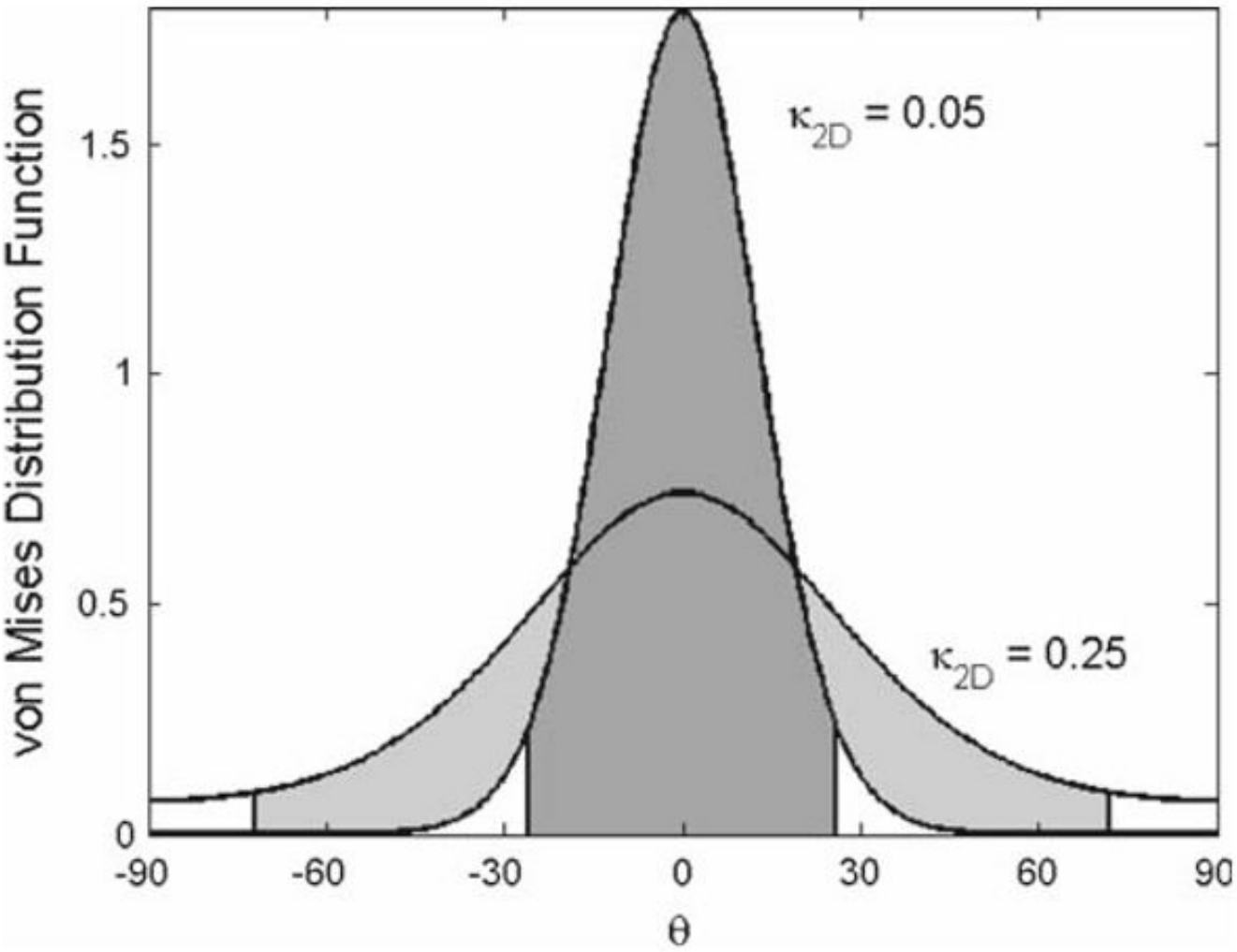

Fig. 2.
The shaded area of the von Mises distribution, for two values of κ_{2D}, represents the angular range in which 95% of fibers are contained

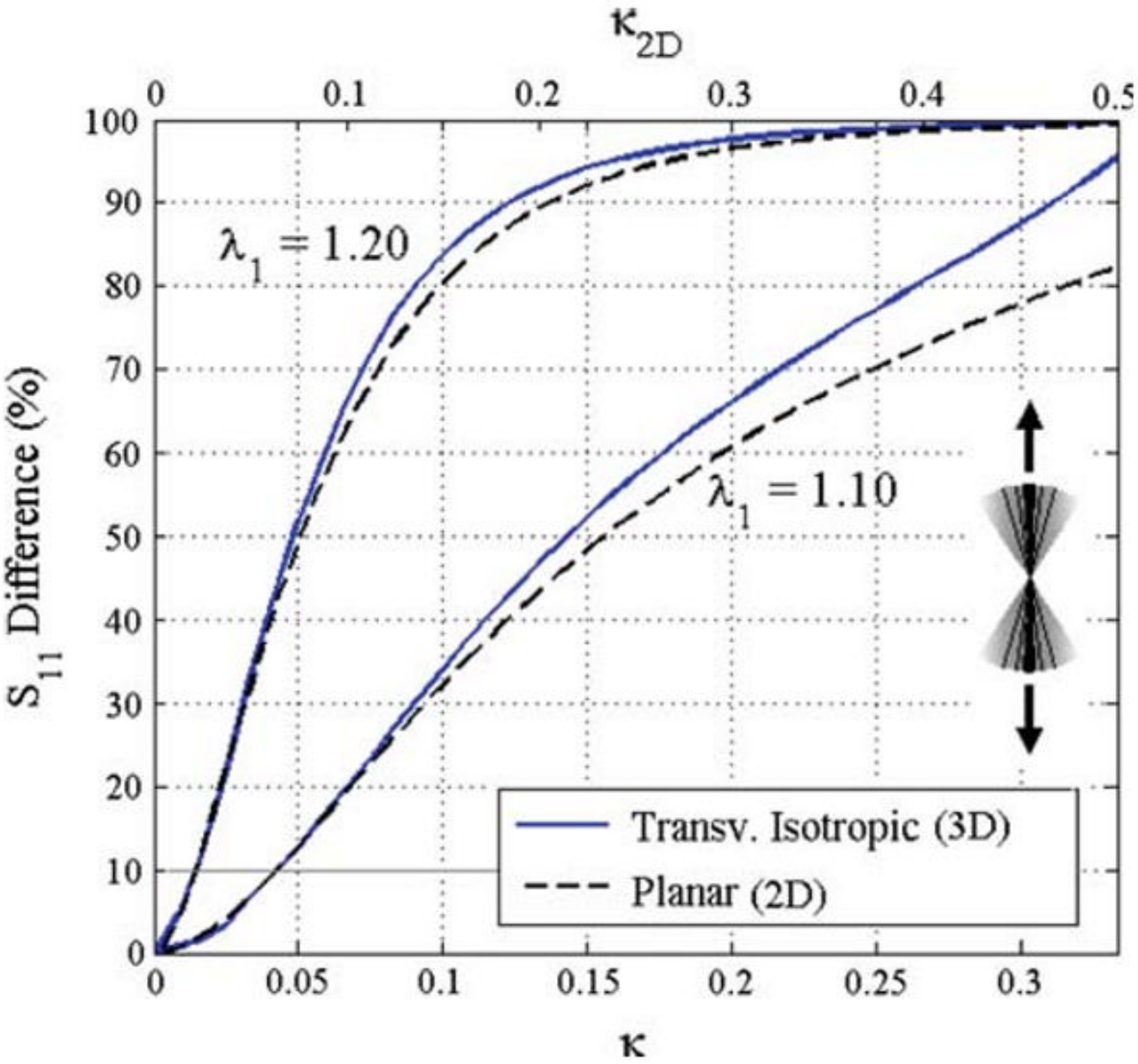

Fig. 3.

Difference of the second Piola-Kirchhoff stresses in the direction $x_1(S_{11})$ between AI and GST formulations increases with the applied stretch (λ_1) and decreases when the fiber distribution (κ for transversely isotropic (3D) and κ_{2D} for planar (2D) distributions) is small. Difference defined as $(S_{AI} - S_{GST})/S_{AI} * 100$. Notice that distributions go from perfectly aligned ($\kappa = \kappa_{2D} = 0$) to isotropic ($\kappa = 1/3, \kappa_{2D} = 1/2$)

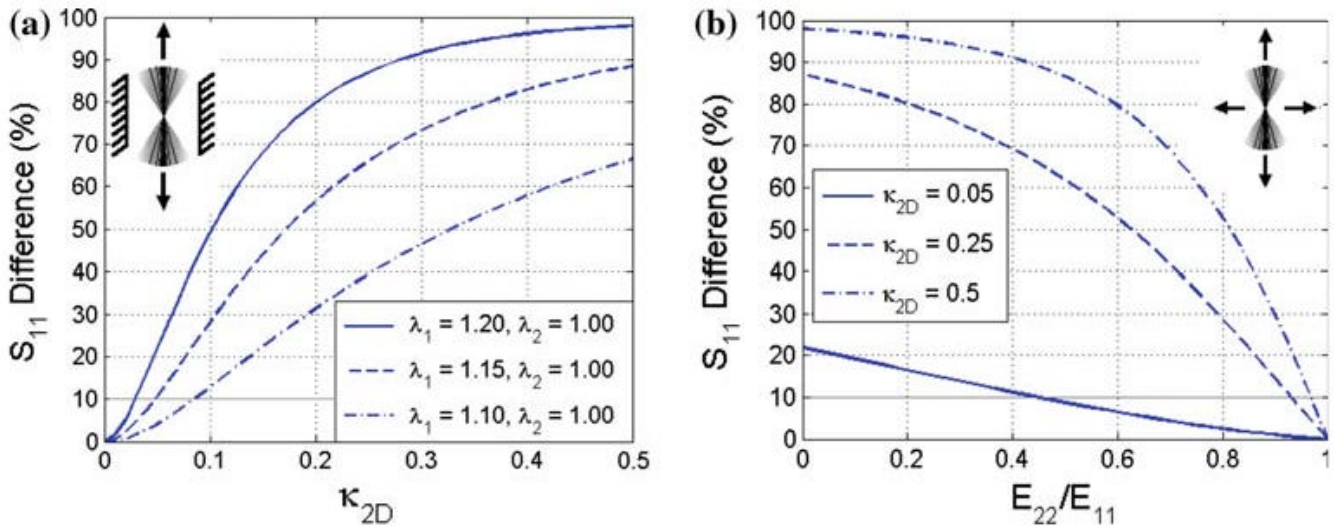

Fig. 4.

A planar family of fibers under biaxial tension: **a** difference of second Piola-Kirchhoff stress in the direction $x_1(S_{11})$ when displacement in the direction x_2 is constrained shows that both formulations are equivalent for small values of fiber distribution (κ_{2D}), **b** the difference of S_{11} as a function of the Lagrangian strain ratio E_{22}/E_{11} vanishes for the equal-biaxial ($E_{22}/E_{11} = 1$) strain configuration. Difference defined as $(S_{AI} - S_{GST})/S_{AI}*100$

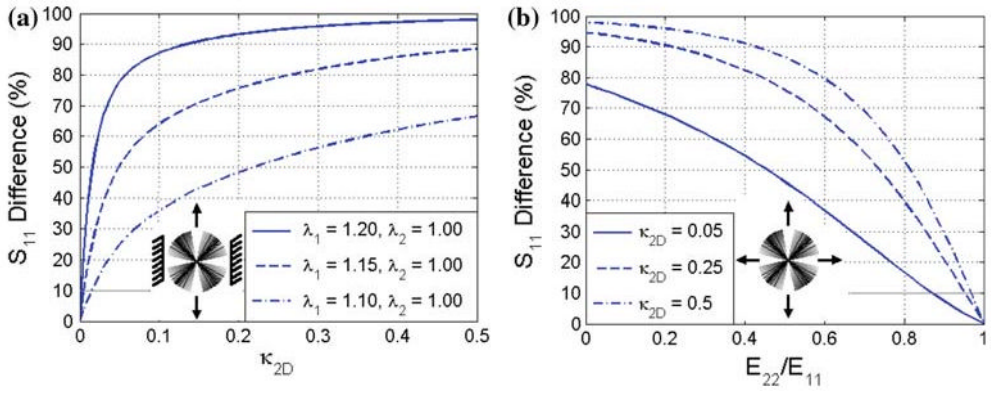

Fig. 5.

Tissue with two planar families of fibers under biaxial tension: **a** difference of second Piola-Kirchhoff stress in the direction x_1 (S_{11}) when displacement in the direction x_2 are constrained shows that both formulations are equivalent for small values of fiber distribution (κ_{2D}), **b** the difference of S_{11} as a function of the Lagrangian strain ratio E_{22}/E_{11} vanishes for the equal-biaxial ($E_{22}/E_{11} = 1$) strain configuration. Difference defined as $(S_{AI} - S_{GST})/S_{AI}*100$

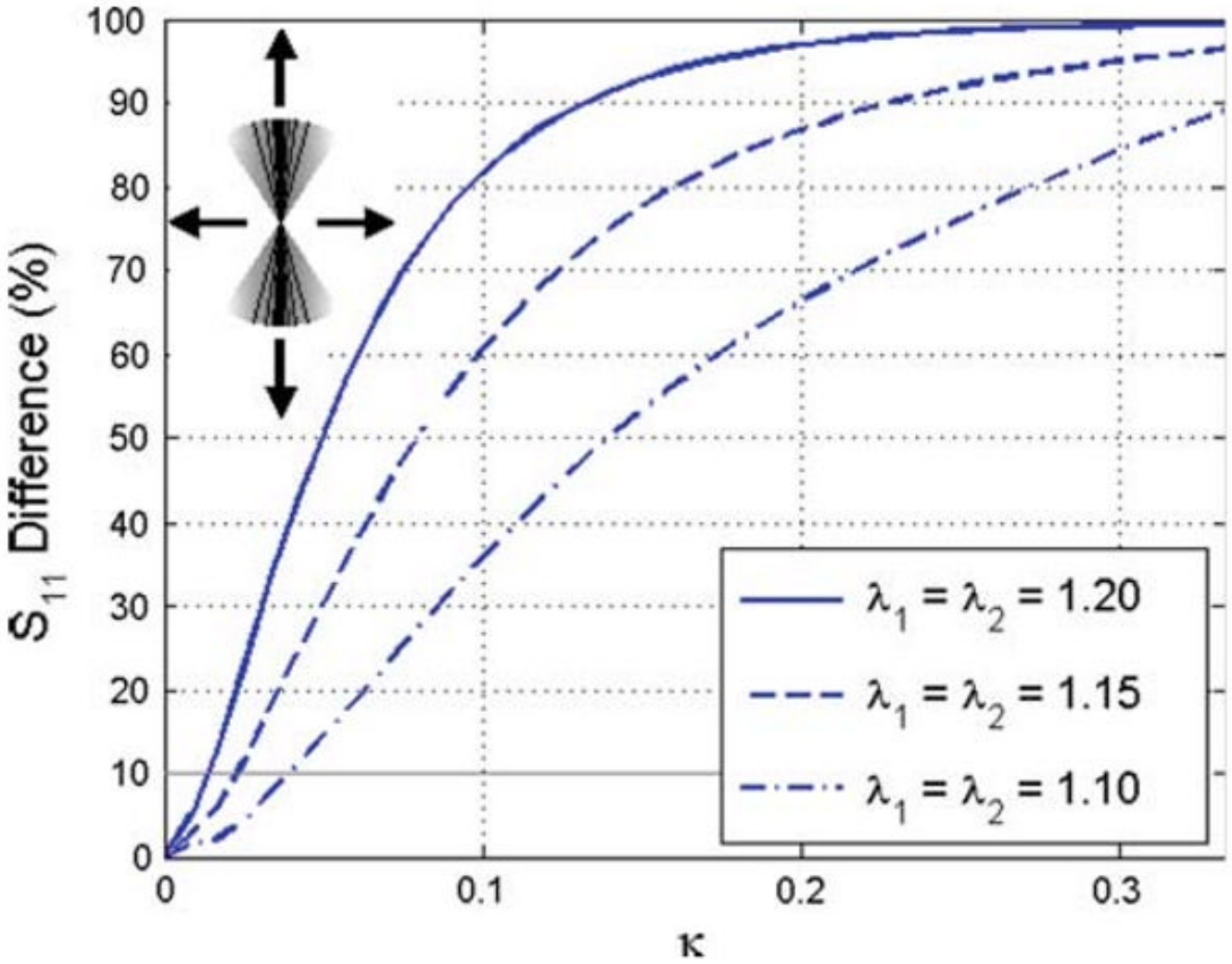

Fig. 6.

Transversely isotropic (3D) family of fibers shows differences in the second Piola-Kirchhoff stresses (S_{11}) even for the case equal-biaxial testing. Difference defined as $(S_{AI} - S_{GST})/S_{AI}*100$

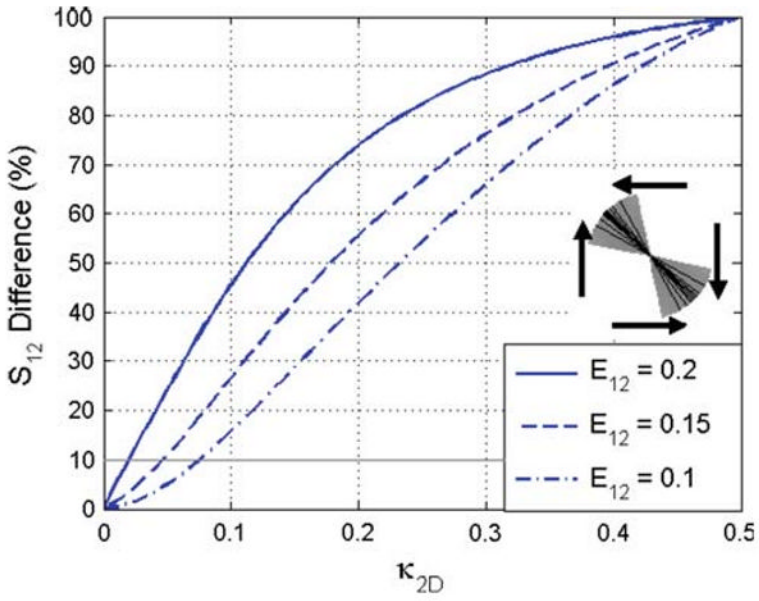

Fig. 7.

Differences between the second Piola-Kirchhoff shear stresses (S_{12}) go from 0 to 100% when the angular distribution (κ_{2D}) increases in a planar family of fibers oriented at 45° from the vertical axis. Difference defined as $(S_{AI} - S_{GST})/S_{AI}*100$